Journal of Pharmaceutical Investigation
https://doi.org/10.1007/s40005-020-00497-6

Online ISSN 2093-6214
Print ISSN 2093-5552

ORIGINAL ARTICLE

Response surface optimization of self nano-emulsifying drug delivery system of rosuvastatin calcium for hepatocellular carcinoma

Nabila M. Sweed[1] · Ahmed M. Fayez[2] · Soad Z. El-Emam[3] · Marwa H. S. Dawoud[1]

Received: 15 April 2020 / Accepted: 21 August 2020

Abstract

Purpose Rosuvastatin calcium (RSC) is a statin which, in addition to its anti-hypercholesteremic effects, was found to have a potential anticancer activity. The target of the present study is to develop self nano-emulsifying drug delivery systems (SNEDDS) loaded with RSC to overcome its poor solubility, and augment its anticancer activity.

Methods A combined mixture-process experimental design was chosen for the optimization of SNEDDS by changing its mixture and process components, where the mixture components were the percentage of Smixture (surfactant and co-surfactant) (X_1) and the percentage of oil (X_2). The process components were the ratio of surfactant to co-surfactant (X_3), and the type of surfactant (X_4). Twenty-four formulae were evaluated for % transmittance and saturated solubility.

Results The optimized formula (O_1) was selected based on the highest % transmittance and highest drug solubility, where the % transmittance was 99.05 ± 0.09% and the saturated solubility was 80.52 ± 2.57 mg/ml. The optimized formula has a globule size of 17.53 ± 0.89 nm, a zeta potential of − 10.2 ± 0.21 mV, and a cloud point of 88.5 ± 0.54 °C. Transmission electron microscopy demonstrated spherical droplet morphology. In vitro drug release showed remarkable increase in the drug release from the optimized formula as compared to the corresponding standard RSC. The anticancer activity of O_1 was evaluated in HepG2 cell-line, where the IC_{50} value was 16.2 ± 0.23 µg/ml. The optimized formula increased cell death by both apoptosis and necrosis.

Conclusion Our results show that the optimized SNEDDS formula is promising for enhancing the anticancer effect of RSC.

Keywords Ternary phase diagram · SNEDDS · Combined mixture and process design · Lipid-based formulation · Solubility improvement · HepG-2 cells

Introduction

Statins are recognized for their effects as anti-hypercholesterolemic agents. Statins block the production of mevalonate (the first step in the cholesterol biosynthesis) by inhibiting HMG-CoA reductase enzyme. The anticancer activity of statins is due to their ability to block mevalonate production, which is produced in high levels in various malignancies such as breast cancer, hepatic cancer, and prostate cancer (Safwat et al. 2017).

Rosuvastatin Calcium (RSC) has a better potent affinity to HMG-CoA reductase active sites than other statins, but it has a poor aqueous solubility, and is extensively metabolized in the liver, leading to a poor bioavailability of 20%. In order to improve the therapeutic performance of RSC, increasing its solubility and avoiding hepatic metabolism is a desirable approach (Balakumar et al. 2013).

Self-nanoemulsifying drug delivery systems (SNEDDS) enhance the oral bioavailability of poorly soluble drugs (Hong et al. 2006), as they spontaneously emulsify forming O/W nanoemulsion, with droplets in the nanorange size. This in turn, improves the oral absorption, and enhances the intestinal permeation of the drug (Wang et al. 2010). It has been reported that SNEDDS formulated using lipids with long chain unsaturated fatty acids effectively solubilize poorly soluble drugs, and increase lymphatic drug transport

✉ Nabila M. Sweed
nsueed@msa.eun.eg; nabila.msweed@gmail.com

[1] Department of Pharmaceutics, Faculty of Pharmacy, October University for Modern Sciences and Arts, Giza, Egypt

[2] Department of Pharmacology, Faculty of Pharmacy, October University for Modern Sciences and Arts, Giza, Egypt

[3] Department of Pharmacology & Toxicology, Faculty of Pharmacy, October 6 University, Giza, Egypt

Published online: 02 September 2020

(Lind et al. 2008). SNEDDS have been reported to inhibit p-glycoprotein mediated drug efflux (Date et al. 2010; Seo et al. 2013).

The present study aims to formulate and optimize SNEDDS loaded with RSC, in an attempt to overcome the low solubility and the low bioavailability (~20%) of RSC (Tripathi et al. 2018), and to enhance its anticancer activity.

Materials and methods

Materials

Rosuvastatin Calcium was generously supplied by Global Napi Pharmaceuticals (Cairo, Egypt). Olive oil and Cinnamon oil were purchased from S.D. Fine Chemicals (Mumbai, India). Labrafil® M 1944 CS (oleoyl polyoxyl-6 glycerides), Labrafac® Lipophile WL 1349 (caprylic capric triglyceride), Labrasol® (caprylocaproyl macrogol-8 glycerides), Peceol® (glyceryl monoloeate), Transcutol® P (diethylene glycol monoethylether) were supplied as generous gifts from Gattefosse (Saint-Priest, France). Tween® 80 (polysorbate 80) and hydrochloric acid (HCl) were purchased from Merck (Darmstadt, Germany). Span 20® was purchased from Sigma Aldrich (St. Louis, USA). Methanol (HPLC grade) was purchased from Riedel-de Haen (Gmbh, Germany). Doxorubicin and the reagents used to maintain cell culture were procured from Sigma (MO, USA). All other chemicals and solvents were of analytical grade and were used without further purification.

Cell line

Human hepatocellular carcinoma cells (HepG2) were purchased from the American Type Culture Collection (ATCC, USA). HepG2 cells were cultured in RPMI supplemented with 10% fetal bovine serum, 100 µg/ml streptomycin and 100 units/ml penicillin, in a humidified atmosphere of 95% air and 5% CO_2 at 37 °C.

Screening of different oils, surfactants and co-surfactants for SNEDDS formation

The saturated solubility of the drug in different oils, surfactants and co-surfactants was done by adding one gram of the drug to two grams of the selected vehicles, into screw capped glass vials. The vials were then shaken at 100 rpm for 72 h in a thermostatically-controlled shaking water bath, which was kept at 25 ± 0.5 °C bath (incubator shaker, ZHWY-2102C, Shanghai, China). After reaching equilibrium, the samples were centrifuged at 5000 rpm for 30 min, followed by filtration through a Millipore® membrane filter (0.45 µm) (Fahmy et al. 2014). The filtrates were diluted with methanol, and quantified spectrophotometrically (UV–1700, Shimadzu, Tokyo Japan) for the dissolved drug, at the predetermined wavelength of 244 nm. Each measurement was carried out in triplicate (Ujilestari et al. 2018).

Construction of ternary phase diagrams

For the development of the ternary phase diagrams, water titration method was used to determine the self nano-emulsifying region. The total of surfactant, co-surfactant, and oil concentrations were always made to be 100%. The components were mixed for 5 min using a magnetic stirrer (Jenway 1000, Barloworld Scientific, Essex, UK), then titrated with distilled water, and agitated once again using the magnetic stirrer. The mixtures were then equilibrated in a thermostatically controlled shaker at 25 ± 2 °C, and were visually assessed for the final appearance of the emulsion. Only clear or slightly bluish dispersions were considered in the nanoemulsion region of the diagram (Basalious and Abdallah Ahmed 2017). The results were plotted to draw the ternary phase diagram using SigmaPlot® 12.5.0.38 software (Systat Software, San Jose, CA, USA).

Preparation of rosuvastatin Ca-loaded SNEDDS

After identification of the self-nanoemulsifying region, SNEDDS were prepared using different ratios of components. RSC was first dissolved in the surfactant/co-surfactant mixture (Smix), and mixed for 2 min using the vortex mixer (SA8, Staffordshire, UK), after which the oily phase was added. Mixing was again continued till a homogenous mixture was obtained. SNEDDS formulae were stored in screw-capped glass vials at 25 °C.

Optimization of the SNEDDS formulae using combined mixture-process experimental design

A combined mixture-process experimental design was chosen for the optimization of SNEDDS as it was reported to reduce the variance associated with the estimates of the coefficients in the model (Isailović et al. 2016). The mixture components were based on a two-component system, namely the amount of Smix (surfactant and co-surfactant) (X_1) and the percentage of oil (X_2), with the sum of their proportions restricted to 100%. The process components were set to be the ratio of surfactant to co-surfactant (X_3), and the type of surfactant used (X_4), which were both set at two levels as shown in Table 1. Based on preliminary trials and the ternary phase diagrams, some additional constraints were placed on the proportions of mixture components, where Smix (X_1) was set between 50 and 90%, and oil % (X_2) was set between 10 and 50%. Due to these limitations, no mixture component was tested "pure." On the contrary, the

Table 1 Mixture and process factors of RSM with their levels

Factor	Type	Low level (− 1)	High level (+ 1)
SAA/CoSAA Mix (Smix) (%) (X_1)	Mixture factors	10	50
Oil (%) (X_2)		50	90
SAA:CoSAA (X_3)	Process factors	1:1	2:1
Type of SAA (X_4)		Tween 80 (T80)	Labrasol (L)

process variables were varied independently of one another, and of the mixture components.

Crossing a classical 2^2 factorial arrangement with a two-component simplex-centroid mixture design was done to construct the combined mixture-process experimental design, in order to analyze the desired responses. According to the applied response surface design, 24 experimental runs were suggested by the design and randomly performed. The measured responses were, the % transmittance (Y_1) and the saturated solubility (Y_2) of the prepared SNEDDS, which were both evaluated as tabulated in Table 2. The aim of the optimization was the preparation of RSC-loaded SNEDDS with the highest % transmittance and saturated solubility as well. The significant factors were taken into consideration while the non-significant factors were not.

A numerical and a graphical optimization were applied to determine the optimum levels for mixture and process variables, in order to get the desired responses of interest using Design-Expert® 10.0.1.0 software (Stat-Ease Inc., USA). The RSC-loaded SNEDDS formula with the highest desirability was subjected to further investigation.

The best fitting mathematical model from linear, quadratic and special cubic models, was selected based on the comparisons of some important statistical parameters such as the standard deviation (SD), the multiple correlation coefficient (R^2), the adjusted multiple correlation coefficient (adjusted R^2), and the predicted residual sum of square (Basalious et al. 2010).

Table 2 Composition of the prepared formulae and their measured responses

	S Mix % (X_1)	Oil % (X_2)	SAA:CoSAA (X_3)	SAA type (X_4)	% Transmittance (Y_1)	Saturated solubility (Y_2)
F1	90	10	1:1	T80	99.1380 ± 0.134	84.5147 ± 0.630
F2	75	25	1:1	T80	42.6580 ± 0.096	59.9063 ± 0.098
F3	90	10	2:1	L	97.2820 ± 0.843	45.0968 ± 0.804
F4	50	50	1:1	L	63.0957 ± 0.456	54.6728 ± 0.156
F5	50	50	1:1	L	18.1552 ± 0.187	55.3409 ± 0.034
F6	50	50	1:1	T80	9.2683 ± 0.215	59.5722 ± 0.190
F7	50	50	2:1	L	43.3511 ± 0.156	39.1952 ± 0.154
F8	50	50	1:1	T80	52.7230 ± 0.098	59.3496 ± 0.198
F9	75	25	2:1	L	13.6773 ± 0.056	41.7563 ± 0.078
F10	75	25	2:1	T80	68.5488 ± 0.076	54.8956 ± 0.198
F11	90	10	2:1	T80	99.8030 ± 0.154	65.6965 ± 0.074
F12	90	10	1:1	L	82.0310 ± 0.630	91.3070 ± 0.034
F13	75	25	1:1	L	12.3027 ± 0.198	42.4243 ± 0.209
F14	50	50	2:1	T80	10.6660 ± 0.078	44.8740 ± 0.187
F15	90	10	2:1	L	97.0620 ± 0.034	44.7627 ± 0.056
F16	75	25	1:1	T80	38.2825 ± 0.189	61.2425 ± 0.032
F17	75	25	2:1	T80	45.3942 ± 0.198	54.4502 ± 0.276
F18	75	25	1:1	L	1.1350 ± 0.034	41.7563 ± 0.309
F19	90	10	2:1	T80	99.7240 ± 0.089	65.8079 ± 0.023
F20	90	10	1:1	L	98.6190 ± 0.187	90.1935 ± 0.210
F21	50	50	2:1	T80	58.8844 ± 0.198	45.4308 ± 0.187
F22	50	50	2:1	L	14.8936 ± 0.198	39.8633 ± 0.198
F23	75	25	2:1	L	0.7447 ± 0.089	40.0860 ± 0.076
F24	90	10	1:1	T80	99.5150 ± 0.254	81.9536 ± 0.093

Data are given as mean ± SD (n = 3)

Characterization of the prepared rosuvastatin Ca-loaded SNEDDS

Determination of the percentage transmittance

In order to determine the % transmittance, one ml of each SNEDDS formula was diluted with deionized water (1:1000), and measured spectrophotometrically at 638.2 nm, using double distilled water as a blank. Each determination was done in triplicate, and the average % transmittance ± SD was calculated (Senapati et al. 2016; Umeyor et al. 2016).

Determination of RSC saturated solubility in the prepared SNEDDS

In screw-capped glass vials, one gram of RSC was added to two grams of each of the prepared SNEDDS formulae. The vials were kept in a constant temperature water bath at 37 ± 0.5 °C, for 72 h, till they reached equilibrium. The formulae were then subjected to centrifugation at 5000 rpm for 30 min, followed by filtration using a Millipore® membrane filter (0.45 µm). The filtrates were diluted with methanol, and measured spectrophotometrically at 244 nm against plain SNEDDS as blank, in order to cancel any interference. The experiment was done in triplicate (El-Laithy et al. 2015).

Thermodynamic stability studies

Centrifugation study The optimized formula (O_1) was visually checked for creaming, cracking, coalescence, phase separation, and phase inversion, after centrifugation at 5000 rpm for 30 min. (Kassem et al. 2016).

Heating and cooling cycle The optimized formula (O_1) was visually checked for creaming, cracking, coalescence, phase separation, and phase inversion, after subjecting the formula to three cycles of 4 °C followed by 45 °C, and storage at each temperature for 48 h (Kassem et al. 2016).

Determination of zeta potential, mean droplet size, and polydispersity index

The optimized formula (O_1) was diluted with double distilled water in the ratio of 1:100 before measuring the zeta potential, mean droplet size, and polydispersity index of the nano-emulsions, using a Zetasizer Nano ZS (Malven Zetasizer version 6.20 serial number: MAL 104 4595, Worcestershire, United Kingdom) (Basalious and Abdallah Ahmed 2017).

Transmission electron microscopy (TEM)

The optimized formula (O_1) was tested with TEM (Ted Pella, Redding, CA) for detection of its morphology, after dilution with double distilled water (1:50). A drop was placed on a carbon-coated copper grid and air-dried for 10 min at room temperature. The excess was removed with filter paper. Phosphotungstic solution 1% (w/v) was used to negatively stain the sample for 30 s.

Cloud point determination

The optimized formula (O_1) was diluted with double distilled water in the ratio of 1:100, and heated gradually in a water bath. The samples were visually assessed for optical transparency, signs of phase separation, and drug precipitation (Hoshtari et al. 2010).

In vitro release studies in different media

A suitable amount of O_1 formula equivalent to 10 mg RSC, was filled into the body of hard gelatin capsules (size 00 elongated) (El-Laithy et al. 2015). The capsules were allowed to solidify for 24 h before use. In order to study the effect of food on the release profile of RSC, different release media were used. The release was done in 500 ml of each of the following: fasted-state simulated gastric fluid (FaSSGF) (pH 1.6), fed-state simulated gastric fluid (FSSGF) (pH 5), fasted-state simulated intestinal fluid (FaSSIF) (pH 6.5) and fed-state simulated intestinal fluid (FSSIF) (pH 5.8), using a USP dissolution tester, apparatus II (Hansson research, USA) at 37 ± 0.5 °C, with 50 rpm (Jantratid et al. 2008). Four ml samples were withdrawn at predetermined time intervals through a Millipore® membrane filter (0.45 µm), where they were replaced with equivalent fresh dissolution medium, to maintain sink conditions, for 60 min. The release of RSC from the optimized SNEDDS formula was compared with the standard RSC containing the same drug quantity. RSC concentrations were determined spectrophotometrically at predetermined $\lambda_{max} = 240.5$ nm. The test was conducted in triplicate.

Stability study of rosuvastatin Ca-loaded SNEDDS

The physical stability of the optimized formula was assessed during storage at 25 °C for 6 months. Sealed glass vials containing 5 g of O_1 were examined visually for potential precipitation of RSC on a regular basis. In addition, % transmittance and drug content were measured as mentioned earlier.

In vitro cytotoxicity studies

In vitro assay for anticancer activity (MTT Assay) The antiproliferative activity of the standard RSC, optimized (O_1) formula, and blank formula (same composition of the optimized formula but without the drug) towards the human hepatocellular carcinoma cells, HepG2 cell line, was evaluated by MTT ((3-[4, 5-dimethylthiazol-2-yl]-2, 5 diphenyl tetrazolium bromide)) assay as that used by Mosmann (Mosmann 1983). HepG2 cells (0.5×10^5) were seeded in 96-well culture plate in 180 µl/well RPMI media augmented with 10% fetal bovine serum, 2 µmol/ml L-glutamine, 250 ng/ml fungizone, 100 units/ml penicillin streptomycin solutions at 37 °C in a CO_2 incubator. Cells were allowed to settle down by incubating them for 24 h at 37 °C in a humidified 5% CO_2 atmosphere. Cells were then treated with 20 µl of different concentrations of standard RSC, blank formula, O_1 formula (100–3.123 µg/ml), or doxorubicin (DOX) as a positive standard drug. The plates were then incubated at 37 °C in a humidified 5% CO_2 atmosphere for 24 h. MTT solution 40 µL/well was then added and incubation was continued for 4 h. Acidified isopropanol was added to solubilize MTT crystals, then microplate ELISA reader (FLUOstar Omega, BMG, Labtech, Germany) was used for the photometric determination of the absorbance at 570 nm. The median growth inhibitory concentration (IC_{50}) was determined by using a GraphPad Prism®, version 5.01 (California Corporation, USA).

Cellular uptake studies and flow cytometric analysis The formula with maximal cytotoxicity from the MTT assay was selected to evaluate its effect on HepG2 cell line. In a six-well culture plate, HepG2 cells were treated with standard RSC and O_1 formula using half the concentration of the IC_{50} for 24 h, then the cells (10^5 cells) were collected by trypsinization and washed twice with ice-cold phosphate buffer saline (PBS) of pH 7.4. Ice-cold ethanol (60%) was used to re-suspend the cells, which were fixed by incubation at 4 °C for 1 h. Phosphate buffer saline (pH 7.4) was used for washing the fixed cells twice, where they were re-suspended in 1 ml of PBS containing 50 µg/ml RNAase A and 10 µg/ml propidium iodide (PI). These cells were further incubated for 20 min in dark at 37 °C. The cells were then analyzed for DNA content, using flow cytometry analysis (ACEA Novocyte™ flowcytometer, ACEA Biosciences Inc., San Diego, CA, USA). ACEA NovoExpress™ software (ACEEA Biosciences Inc., San Diego, CA, USA) was used to calculate cell cycle distribution. DOX was used as a positive standard.

Assessment of apoptosis In order to detect apoptosis and necrosis, Annexin V-FITC apoptosis detection kit (Abcam Inc., Cambridge Science Park, Cambridge, UK) was used, coupled with 2 fluorescent-channel flow cytometry.

After cell treatment with standard RSC and O_1 formula, using half the concentration of the IC_{50} for 24 h, trypsinization was used to collect cells (10^5 cells), which were then washed twice with ice-cold PBS (pH 7.4). Incubation of the cells with 0.5 ml of Annexin V-FITC/PI solution was done at room temperature and in the dark, for 30 min. The cells were then injected via ACEA Novocyte™ flow cytometer (ACEA Biosciences Inc., San Diego, CA, USA), and analyzed for FITC and PI fluorescent signals using FL1 and FL2 signal detector, respectively (λex/em 488/530 nm for FITC and λex/em 535/617 nm for PI). Cells were quantified by quadrant analysis and calculated using ACEA NovoExpress™ software.

Statistical analysis

All results were expressed as mean ± SD. Wherever applicable, statistical significance was evaluated using a one-way ANOVA test, where statistical significance was considered at $p < 0.05$ level, using Design-Expert 10.0.1.0 software (Stat-Ease Inc., USA). Parameters of cytotoxicity measurements were evaluated using one-way ANOVA, followed by Tukey's post hoc test ($p < 0.05$) using GraphPad Prism®, version 5.01. (California Corporation, USA).

Results and discussion

Solubility studies

Solubility studies were done to select the best oily phase, surfactant, and cosurfactant. For achieving optimum drug loading, the selection of a suitable oil that best solubilizes the drug is very crucial (Savjani et al. 2012). Another importance of the solubility study is to decrease the total volume of the formula to be administered (Prajapat et al. 2017). In this study, Peceol®, olive oil, and cinnamon oil were the oils of choice. Tween 80®, Span 20®, Labrasol®, and Labrafil® M 1944 CS were the surfactants of choice, and Transcutol® P and PEG400 were the cosurfactants of choice.

The solubility of RSC in different oils, surfactants, and co-surfactants is presented in Table 3. Among the oils, the highest solubility of RSC was in Peceol® (114 ± 1.43 mg/ml), whereas the least solubility was in olive oil (12.57 ± 0.57 mg/ml). Peceol®, therefore, was selected as the oily phase due to its best solubilizing capability for RSC. Peceol® also enhances lymphatic drug transport due to its structure, as it is made up of a long-chain unsaturated fatty acid (Nankervis et al. 1996; Risovic et al. 2004). The long chain fatty acid is also helpful in enhancing the distribution of RSC to the lymphatic system, which in turn improves RSC oral bioavailability, by avoiding its hepatic first pass effect (Garg et al. 2016). The high solubility of RSC in

Table 3 Solubility of RSC in different vehicles

Type of vehicle	Saturated solubility (mg/ml) ± SD, n = 3
Cinnamon oil	12.8 ± 0.43
Peceol®	114 ± 1.89
Labrafac® Lipophile WL 1349	35.8 ± 0.98
Labrafil® M 1944 CS	38.22 ± 1.67
Labrasol®	299.99 ± 3.67
Span 20®	237.17 ± 2.89
Tween 80®	478.8 ± 4.78
Transcutol® P	590 ± 2.45
PEG 400	469.8 ± 5.87

Peceol® was expected, since a lipophilic drug such as RSC (log P = 4.19) is likely to exhibit greater solubility in long-chain lipids, as compared to medium-chain lipids (Shahba et al. 2012).

The use of non-ionic surfactants in this study was attributed to their low toxicity, greater biocompatibility, and being not so much affected by the change in pH and ionic strength throughout the GIT (Shafiq et al. 2007; Nepal et al. 2010). Among the various surfactants, Tween® 80 (478.8 ± 12.35 mg/ml) and Labrasol® (299.99 ± 9.55 mg/ml) showed the highest solubility of RSC, while Labrafac® Lipophile WL 1349 showed the least solubility among the surfactants (35.8 ± 1.69 mg/ml). In addition, Labrasol® and Tween ®80 were reported to have bio-enhancing activities, including the inhibitory effects on P-gp mediated efflux and CYP450 enzymes (Buggins et al. 2007; Chen 2008). A previous study reported that Tween 80® is an ideal lymphotropic vehicle, and is used to enhance lymphatic absorption (Tripathi et al. 2018). Labrasol®, in addition, was also reported to inhibit enterocytes mediated efflux to the intestinal lumen, thus enhancing the intestinal absorption of drugs (Balakumar et al. 2013; AboulFotouh et al. 2017).

Co-surfactants were reported to stabilize nano-emulsion by decreasing the interfacial tension, and to guard against coalescence formation, as they form a mechanical barrier (Shahba et al. 2012). As shown in Table 3, both co-surfactants, Transcutol® P and PEG 400 showed good solubilization capacity for RSC, where the solubility of RSC was 590 ± 15.77 mg/ml and 469.8 ± 11.43 mg/ml, respectively.

The combination of a surfactant with a high HLB and a co-surfactant with a low HLB, was reported to rapidly form a stable nano-emulsion when dispersed in water. For this reason, Tween 80® and Labrasol® (HLB 15 and 14, respectively) and Transcutol® P (HLB 4) were selected as the surfactant mixture in this study. As Transcutol® P is known for its good solving power, it was chosen as a co-surfactant in this study, in order to maximize RSC loading capabilities, and to enhance its permeability (Zhao et al. 2010). Transcutol ®P was reported to increase the drug loading and self dispersibility of SNEDDS (Hong et al. 2006; Shen and Zhong 2006).

Construction of ternary phase diagram

According to the preliminary screening results, Peceol ® was used as the oil phase, Tween® 80 and Labrasol® were used as the surfactants, and PEG 400 and Transcutol ® P were used as the co-surfactants, for constructing different phase diagrams. Five phase diagrams were constructed, as represented in Fig. 1. The shaded area represents the self-nano-emulsion region, where SNEDDS emulsify spontaneously under gentle agitation. The larger the area of emulsification, the better the self-nano-emulsifying ability (Elnaggar et al. 2009).

As shown in Fig. 1, phase diagrams prepared using Tween 80® or Labrasol ® as surfactants, and Transcutol® P as co-surfactant, yielded a good nano-emulsification region. This is because of the high HLB of both Tween 80® (HLB = 15) and Labrasol ® (HLB = 14), and the solubilizing effect of Transcutol® P. It was observed that there was almost no difference in the width of the nano-emulsification region between ternary phase diagrams constructed using Tween 80® and Labrasol® (Parmar et al. 2011). Surfactants stabilize nano-emulsion by providing a mechanical barrier to coalescence, as well as by reducing the interfacial energy. Transcutol® P (HLB = 4) increases the interfacial fluidity of the outer surface of surfactants. Moreover; it enhances emulsification when diluted in an aqueous medium (Seo et al. 2013).

It was found that the use of PEG 400 as a co-surfactant resulted in only one phase diagram, using Tween ®80 as a surfactant, and a ratio of SAA: CoSAA of 2:1, with a narrower nano-emulsification region, as compared to those prepared using Transcutol® P as co-surfactant. Therefore, PEG400 was excluded, and only phase diagrams constructed using Transcutol® P as co-surfactant were used in the formulation of the SNEDDS.

Statistical analysis using combined mixture-process experimental design

The optimized SNEDDS formula was selected using a combined mixture-process experimental design. The use of this design allows for simultaneous analysis of the effects of the mixture components and the processing factors. Moreover, it is used to calculate the possible interactions between the tested variables, and finally optimize the formula by both the mixture design and the factorial design (Isailović et al. 2016). The chosen design supported a quadratic-mixture model crossed with a three-factor interaction process model

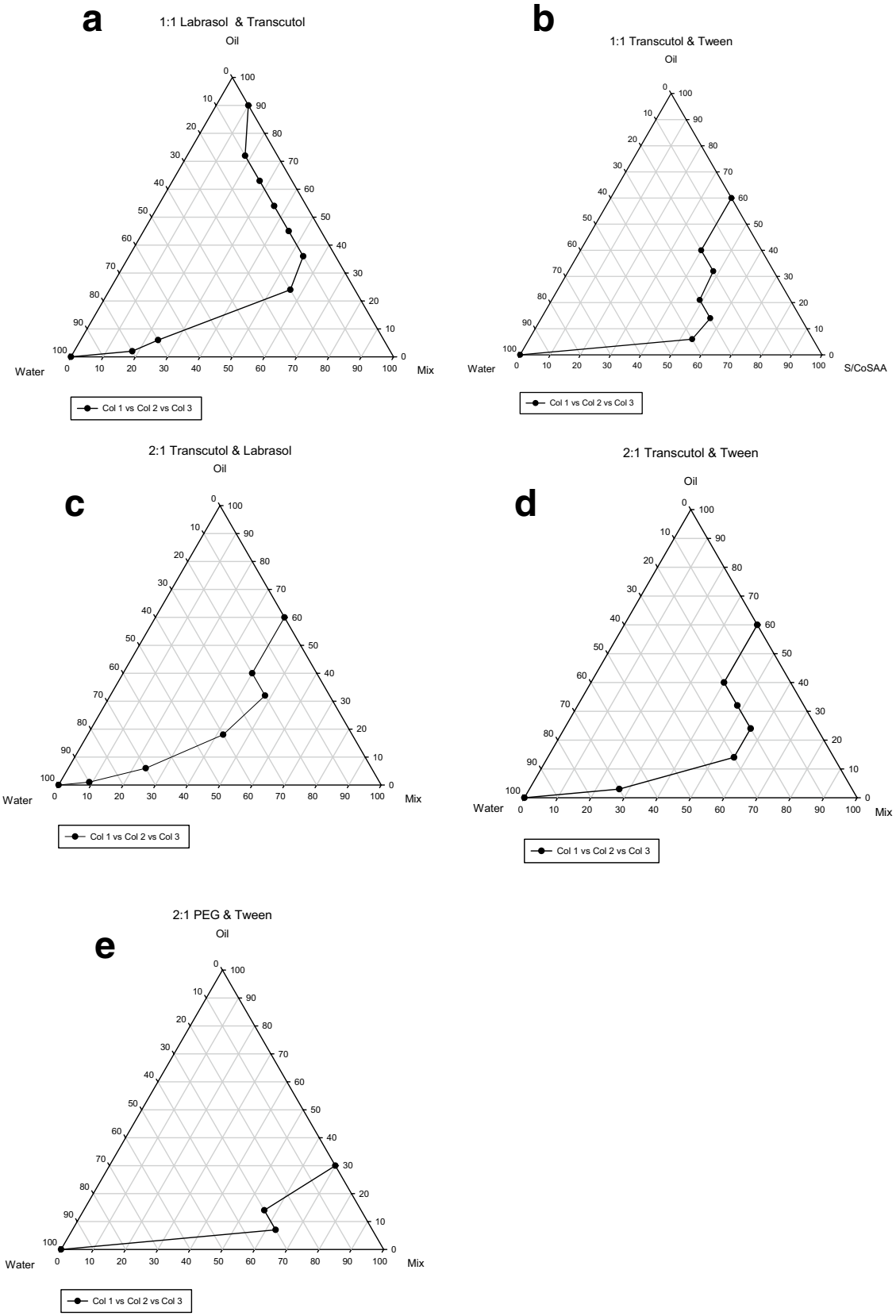

Fig. 1 Ternary phase diagrams using **a** 1:1 Labrasol: Transcutol P, **b** 1:1 Tween 80: Transuctol P, **c** 2:1 Labrasol: Transcutol P, **d** 2:1 Tween 80: Transcutol P and **e** 2:1 Tween 80: PEG400

for both measured responses, namely the % transmittance and the saturated solubility.

Evaluation of these models suggested a good fit, showing significance for both the mixture and the process designs, as evidenced by model F values ($p < 0.0001$), which are represented in Table 4.

Backward method was used to eliminate the insignificant terms, except those required to maintain hierarchy, thus generating reduced regression models for % transmittance and saturated solubility. The regression equations obtained for the responses were as follows:

$$\%\ \text{Transmittance}\ (Y_1) = +96.65 * X_1 + 33.88 * X_2 - 193.14 * X_{12} \quad (1)$$

$$\begin{aligned}\text{Saturated Solubility}\ (Y_2) = {} & +71.17 * X_1 + 49.79 * X_2 - 57.96 * X_{12} \\ & - 15.83 * X_{13} - 3.33 * X_{14} - 7.45 * X_{23} \\ & - 2.52 * X_{24} + 46.57 * X_{123} - 21.48 * X_{124} \\ & - 7.08 * X_{134} - 0.29 * X_{234} + 24.41 * X_{1234}\end{aligned} \quad (2)$$

The fitted models had a high correlation coefficient R^2, an adjusted R^2 in a reasonable agreement with the predicted R^2, and adequate precision values (0.7412, 0.7165, 0.6619, 9.902, for % transmittance, and 0.9988, 0.9977, 0.99752, 93.532 for saturated solubility, respectively), indicating that the models for the two responses can be used to navigate the design space.

A positive sign of coefficient of the numeric factors indicates a synergistic effect, while a negative sign of coefficient indicates an antagonistic effect on the response. A coefficient with a larger value indicates more influence of the factor on the studied response (Isailović et al. 2016).

It has been reported that the measurement of % transmittance of diluted SNEDDS by simple equipment could be an alternative to measuring the particle size by expensive and sophisticated equipment (Basalious et al. 2010). A previous study reported a good correlation between % transmittance and the particle size (Dash et al. 2015). Accordingly, in the present study, the % transmittance of the diluted SNEDDS was measured. A value of % transmittance approaching 100% indicates the clarity and transparency of SNEDDS dispersion, and shows that the particle size is in the nanometer range.

The % transmittance of the prepared SNEDDS formulae ranged from 0.7447% to 99.803% as shown in Table 2.

As shown in Table 4, only X_{12} was a significant model on the % transmittance. It was found that the % transmittance was lowered because oil % (X_2) has an antagonistic effect on the effect of Smix % (X_1), as can be deduced from the negative coefficient of X_{12}. This could be due to the fact that surfactants lower the surface tension, leading to the formation of fine droplets. This, in turn, increases the clarity of dispersion, leading to an increase in % transmittance. Thus, the increase in oil as a mixture component leads to the reduction in Smix %, which causes a reduction in the % transmittance (Krstić et al. 2018). Moreover, Peceol®, as a hydrophobic long-chain triglyceride, produced coarser droplets because it increased the surface tension, which in turn resulted in a decrease in % transmittance (Pouton and Porter 2008).

The saturated solubility of the prepared SNEDDS formulae ranged from 39.19 to 91.30 mg/ml as shown in Table 2, where there is a marked increase in the saturated solubility as compared to the standard drug, which was found to be 8 mg/ml. As shown in Table 4, each of X_{12}, X_{13}, X_{14}, X_{23} and X_{24} were found to be significant antagonistic terms on the saturated solubility.

Table 4 ANOVA table for the measured responses

Source	Sum of squares		DF		Mean square		F-value		P-value	
	%T	Sat. sol	%T	Sat. sol	%T	Sat. sol	%T	Sat. sol	%T	Sat. sol
Model	23,227	6007.87	2	11	11,613.49	546.17	30.07	910.6	< 0.0001	< 0.0001
Linear mixture[a]	12,522	1499.22	1	1	12,521.86	1499.22	32.42	2499.56	< 0.0001	< 0.0001
X_1X_2	10,705	964.15	1	1	10,705.13	964.15	27.72	1607.47	< 0.0001	< 0.0001
X_1X_3		2003.6		1		2003.6		3340.49		< 0.0001
X_1X_4		88.53		1		88.53		147.6		< 0.0001
X_2X_3		443.61		1		443.61		739.6		< 0.0001
X_2X_4		50.77		1		50.77		84.65		< 0.0001
$X_1X_2X_3$		622.52		1		622.52		1037.89		< 0.0001
$X_1X_2X_4$		132.45		1		132.45		220.83		< 0.0001
$X_1X_3X_4$		401.54		1		401.54		669.46		< 0.0001
$X_2X_3X_4$		0.68		1		0.68		1.14		0.3068
$X_1X_2X_3X_4$		170.97		1		170.97		285.05		< 0.0001

[a]Inference for linear mixtures uses Type I sums of squares

It was observed that increasing the oil % (X_2) had an antagonistic effect on the saturated solubility as indicated by the negative coefficient of $X_{12.}$ This might be due to the fact that an increase in oil % is accompanied by a decrease in the Smix % (X_1) which is known to be responsible for the emulsification process (Soltani et al. 2017).

It was observed that increasing the SAA to CoSAA ratio (X_3) had an antagonistic effect on both Smix % (X_1) and oil % (X_2), resulting in a decrease in the saturated solubility. This might be attributed to the relative increase in the SAA amount, and the relative reduction in the CoSAA, leading to the reduction of drug solubility. This is because co-surfactants improve the dispersibility and drug absorption of the formula (Lawrence and Rees 2012; Rahman and Mujahid 2018). Furthermore, using Tween 80® as the surfactant had a synergistic effect on both the Smix% (X_1) and the oil % (X_2), thus enhancing the saturated solubility. The negative coefficient of X_{14} resulted from the negative-coded value of Tween 80®. The higher HLB value of Tween ®80 over Labrasol® indicates a higher hydrophilic property, and thus a faster emulsification power. Also the structure difference and the chain length of both surfactants have attributed to the better effect of Tween ®80 over that of Labrasol® on the saturated solubility (Kassem et al. 2016).

Interaction plots could be used for the interpretation of the interaction between factors. As can be observed from Fig. 2a, b, the % transmittance showed a non-linear relationship with Smix % (X_1), oil % (X_2), and SAA: CoSAA (X_3). An initial decrease in the % transmittance was observed when the Smix % (X_1) was increased and the oil % (X_2) was decreased, using either surfactants. This was followed by an increase in the % transmittance. The decrease in % transmittance at the beginning may be due to the high amount of oil (more than 30%), which resulted in a difficulty in its emulsification, and an increase in particle size, hence a lower % transmittance (Soltani et al. 2017). The increase in % transmittance that followed was due to the decrease in oil to 30%, and the increase in Smix %, using either surfactants. This is

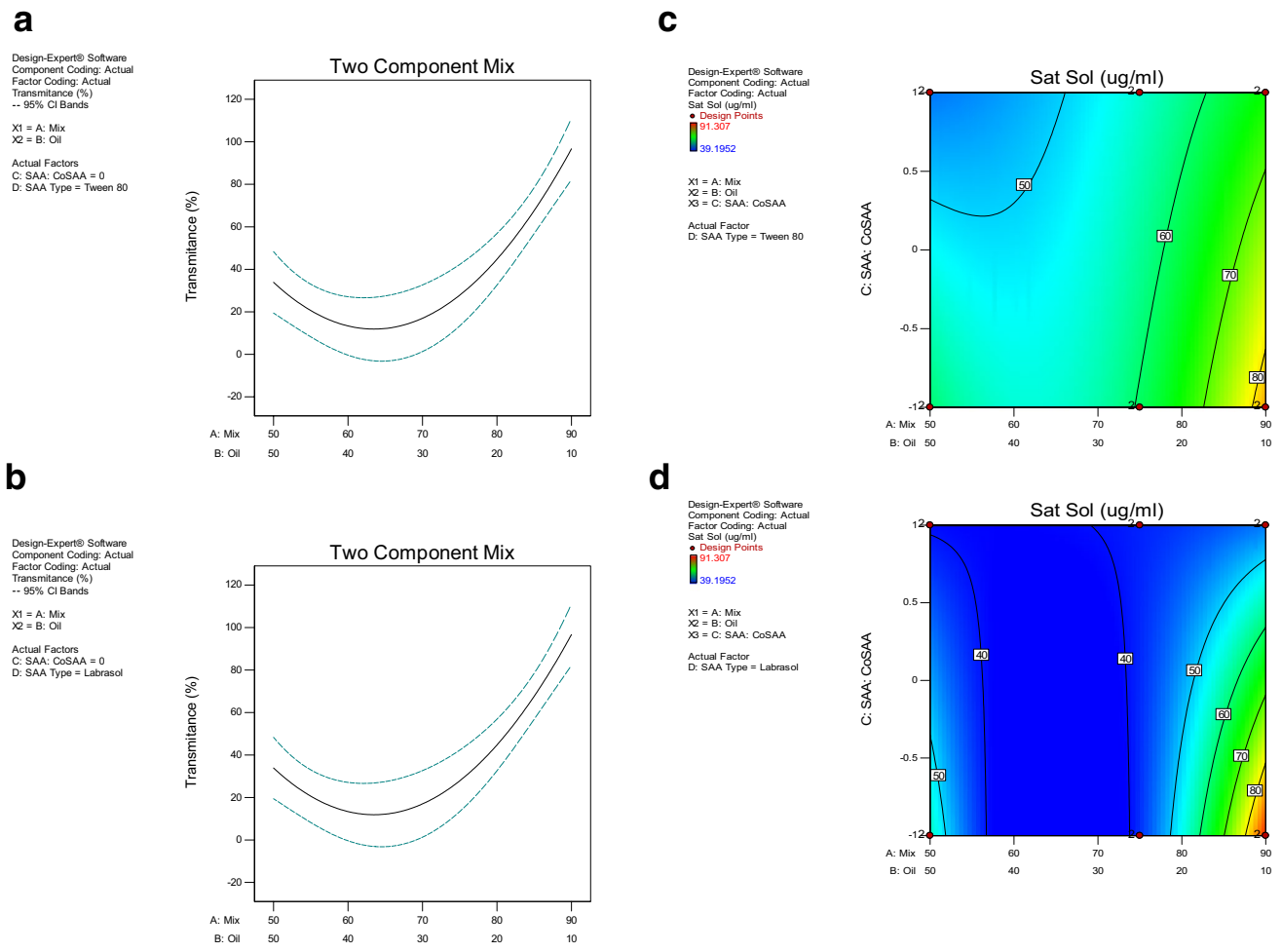

Fig. 2 Interaction plot for the % transmittance, keeping the SAA:CoSAA ratio at its intermediate level using; **a** Tween 80 and **b** Labrasol, Interaction plot for the Saturated solubility using; **c** Tween 80 and **d** Labrasol

due to the ability of Smix to enhance the solublization of the oil component, which in turn leads to a smaller particle size and higher % transmittance (Kommuru et al. 2001; Singh et al. 2010).

Upon using Tween ® 80 as the SAA, the saturated solubility was found to increase as both SAA: CoSAA (X_3) and oil% (X_2) were lowered, and Smix % (X_1) was increased, as shown in Fig. 2c. This could be due to the fact that the increase in Smix % (with the consequence of lowering the oil%) leads to an increase in the emulsification (Kommuru et al. 2001; Singh et al. 2010), which in turn leads to an increase in the saturated solubility. In addition, by lowering the SAA: CoSAA ratio, the amount of CoSAA relatively increases, which leads to better dispersibility as mentioned earlier (Lawrence and Rees 2012; Rahman and Mujahid 2018).

Upon using Labrasol® as the SAA, an initial reduction in the saturated solubility was observed, with a reduction in oil % and an increase in each of Smix % and SAA: CoSAA. This was followed by an increase in the saturated solubility caused by the reduction in both oil % (X_2) and SAA: CoSAA (X_3), and an increase in Smix % (X_1) (Fig. 2d). This may be due to the same reason explained in the case of Tween® 80.

Optimization of SNEDDS

Optimization was done to select the mixture-process combination resulting in drug-loaded SNEDDS with the highest % transmittance and the maximum saturated solubility (Avachat and Patel 2015; Dash et al. 2015).

The composition of the optimized SNEDDS formula, with the predicted and observed responses and desirability, are given in Table 5. An optimized formula was suggested by the program and was found to have 90% Smix, 10% oil, a 1:1 ratio of SAA: CoSAA, and Tween 80® as the SAA, with a desirability of 0.889. The optimized formula was prepared and characterized in terms of % transmittance and saturated solubility, to calculate the % prediction error which was found to be very small as shown in Table 5. Thus, this design could be successfully used for the preparation and optimization of RSC loaded SNEDDS.

The % transmittance of the optimized formula was 99.05 ± 0.09% and the saturated solubility was 80.52 ± 2.57 mg/ml. There was a marked enhancement in RSC solubility (10 folds) in the optimized SNEDDS formula, in comparison to its solubility in water (8 mg/ml). Therefore, around 80 mg of RSC could be encapsulated in 1 ml of SNEDDS formula, which is much greater than the single oral dose of RSC (20 mg).

Characterization

Thermodynamic stability studies

The optimized formula was subjected to centrifugation and to heating and cooling cycles, to check its stability. The optimized formula showed no signs of phase separation or precipitation when centrifuged at 5000 rpm, or when passed under alternative temperature cycles (4 °C and 45 °C), indicating good stability of O_1 formula.

Determination of zeta potential, mean droplet size, and polydispersity index

The mean droplet size of the optimized formula was 17.53 ± 0.89 nm, which is considered ideal for enhancing RSC absorption through lymphatics (Garg et al. 2016). The use of a hydrophilic surfactant (Tween® 80,HLB = 15) with a hydrophobic cosurfactant (Transcutol ®P, HLB = 4), is the reason behind the small droplet size, as they reduce the free energy of the system, leading to the formation of small droplets (Craig et al. 1995).

The polydispersity index (PDI) for the optimized formula was 0.432, which indicates good uniformity of size distribution after dilution with the aqueous phase. Generally, systems with a polydispersity index value greater than 0.5 are considered poly-dispersed systems (Shakeel et al. 2014).

The optimized formula showed a zeta potential value of (− 10.20 ± 0.21 mV). This is due to the non-ionic nature of both Tween®80 and Transcutol® P. However, the small negative zeta potential values of the optimized formula could be due to the ionization of free fatty acids present in the oil (Lu et al. 2008; Cui et al. 2009).

Table 5 The optimized values of the variables with the predicted and observed responses

Optimized formula composition	Response	Predicted value	Observed value	Prediction error%*	Desirability
$S_{mix:}$ 90% Oil%: 10%	Transmittance (%)	96.647	99.05 ± 0.09	2.48	0.889
Surfactant: cosurfactant: 1:1 Surfactant type: Tween 80	Saturated solubility (mg/ml)	83.234	80.52 ± 2.57	3.26	

Data are given as mean ± SD (n = 3)

Prediction error%* = ((Predicted-Observed)/Predicted)*100

Transmission electron microscopy

As shown in Fig. 3, the nanoemulsion droplets appeared as dark spheres against a bright background, with a smooth surface. No sign of aggregation or drug precipitation was observed, which gives a very good indication about the physical stability of the formed nanoemulsions (Badran et al. 2014).

Cloud point determination

The cloud point is an essential parameter for the evaluation of nano-emulsion stability. In order to avoid phase separation in GIT, SNEDDS should have a cloud point higher than the body temperature (Avachat and Patel 2015). The optimized SNEDDS formula showed a cloud point of 88.5 ± 0.54 °C, which indicates the stability of the system that will be formed at the physiological temperature.

In vitro release studies

The Food and Drug Administration (FDA) has stated that RSC administration with food does not affect the area under the curve (AUC) of rosuvastatin (U.S. Food and Drug Administration 2019). However, some authors have reported that the administration of rosuvastatin to healthy volunteers in the fed condition lowered both the C_{max} and AUC significantly, as compared to the fasting state (Li et al. 2007). An earlier study suggested that rosuvastatin should be administered in a fasting state to avoid food effect (Baek et al. 2013). Therefore, in this study, the effect of food on the in vitro dissolution of RSC was examined by simulating the fasting and fed states in both the gastric fluid and the intestinal fluid.

Figure 4 shows the release profile of both the optimized formula and the standard RSC, both containing the same drug amount (10 mg/ml). The release was done in simulated gastric fluid and simulated intestinal fluid in both fasting and fed states. As shown in Fig. 4a, the dissolution profile for the standard RSC in simulated gastric fluid showed 59.28 ± 2.66% vs. 24.28 ± 2.33% drug release after 10 min in the fasting and fed states respectively, with a statistically significant difference (p = 0.0133), whereas by the end of 60 min, 68.17 ± 1.98% vs. 59.73 ± 2.52% of the drug was released in the fasting and fed states, respectively (p = 0.0198).

As shown in Fig. 4b, the dissolution profile for the standard RSC in simulated intestinal fluid showed 78.66 ± 1.30% vs. 70.79 ± 2.40% drug release after 10 min in the fasting and fed states respectively, with a statistically significance difference (p = 0.0133), whereas by the end of 60 min, 96.33 ± 1.77% vs. 90.00 ± 1.22% of the drug was released in the fasting and fed states, respectively (p = 0.0123).

The higher dissolution of RSC in the simulated intestinal fluid is attributed to the nature of the drug. RSC has a pKa of 4.6 (carboxylic acid group), therefore its ionization and hence its solubility was increased in the higher pH medium (Salih et al. 2013). The lower dissolution of RSC in the fed state as compared to the fasting state, confirms the effect of food on lowering the dissolution of RSC as previously reported (Baek et al. 2013).

As shown in Fig. 4, the optimized formula showed higher release as compared to that of RSC in both fasting and fed states, in the simulated gastric and intestinal conditions, where almost 100% of RSC was released after 10 min. The release of RSC from the optimized formula (O_1) was not affected by food or pH. This was due to the entrapment of RSC in nano-emulsion particles, which helps in increasing the rate of the drug dispersal in aqueous media (Abo Enin 2015). These results indicate that the optimized SNEDDS formula successfully increased the RSC solubility, irrespective of the pH of the medium, and also suggest that the incorporation of RSC in SNEDDS could diminish the food effect.

Stability study of rosuvastatin Ca-loaded SNEDDS

The optimized RSC-loaded SNEDDS showed very good stability at 25 °C for six months, as no crystalline drug was observed visually. There was no significant difference in the % transmittance among the fresh and stored samples, where the % transmittance was found to be 99.05 ± 0.62% and 98.71 ± 0.75%, for the fresh and stored samples, respectively (p = 0.5878). The drug content was found to be 80.52 ± 2.57 mg/ml and 79.89 ± 1.98 mg/ml, for the fresh and stored samples respectively (p = 0.4539).

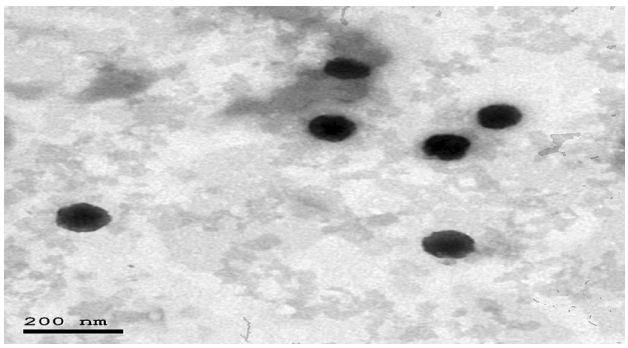

Fig. 3 TEM of the optimized formula

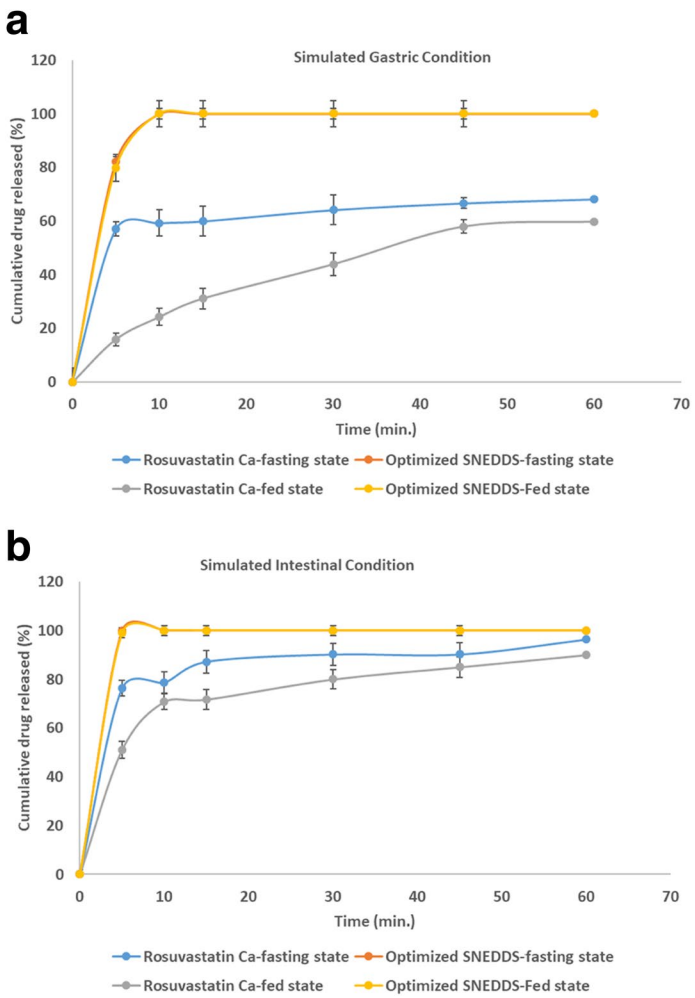

Fig. 4 Release rate of RSC in **a** Simulated gastric condition and **b** Simulated intestinal condition

Evaluation of cytotoxicity in HepG-2 cancer cell line

Statins are reported to be promising anticancer agents, due to their inhibition of the isoprenylation of G-proteins, and the subsequent alteration of downstream signaling pathways. Statins also induce apoptosis, inhibit cell growth and angiogenesis (Mekhail et al. 2012).

The anticancer effect of the standard RSC, the blank formula, and the optimized formula (O_1) was evaluated using MTT assay, and compared to that of untreated cells (control group) that represent 100% of cell viability. DOX was used as a positive standard. The cytotoxicity of the tested samples was evaluated on hepatocellular carcinoma (HepG2) cell line. The blank formula showed no cytotoxic effect over the entire range of concentrations, which indicated the safety of the SNEDDS. As shown in Table 6, O_1 formula showed a statistically significant cytotoxicity with IC_{50} value of 16.2 ± 0.23 µg/ml, when compared to that of RSC (166.8 ± 5.33 µg/ml), where $p < 0.05$, indicating an enhanced cytotoxicity against HepG2 cells ($p < 0.05$). This could be due to the presence of the non-ionic surfactant (Tween 80®) in O_1 formula, which might have enhanced the membrane fluidization, consequently increasing cell permeability (Shukla et al. 2017). In addition, Tween 80® was reported to inhibit P-gp efflux pump, hence increasing the uptake and the cytotoxicity of O_1 formula on HepG2 cells (Buggins et al. 2007). The anticancer effect of the drug was augmented by the lipophilic nature of the SNEDDS, which helped in RSC absorption and facilitated its permeability across the cell membrane (Sandhu et al. 2015). These results are similar

Table 6 The IC_{50} values of RSC, O_1 formula and DOX as positive standard

Sample	IC_{50} value (µg/ml)
RSC	166.8 ± 5.33
O1	16.2 ± 0.23*
DOX	1.3 ± 0.01

Data are given as mean ± SD (n = 3)

*Statistically significant, $p < 0.05$

to those reported by Aldalaen et al. (2019), where the anticancer activity of RSC was highly potentiated when formulated as nano-capsular systems, owing to the high cellular internalization capacity of nano-capsules, due to their lipophilic nature (Aldalaen et al. 2019).

Cell cycle progression by flow cytometric analysis

It was documented that among the anticancer properties of statins is their ability to halt the cell-cycle progression in cancer cells, which in turn reduces the risk of cancer recurrence (Ciofu 2012). By flow cytometric analysis of cell cycle using the PI/RNase staining solution for quantification of DNA content under each phase of the cell cycle, O1 formula induced cell cycle growth arrest of HepG2 cells. As shown in Fig. 5, treatment of HepG2 cells with O_1 formula using half the concentration of IC_{50}, for 24 h, induced a marked arrest in G1 phase. This is unlike HepG2 cells treated with DOX as a positive standard, which showed a significant arrest in S phase as well as G2/M phase, when compared

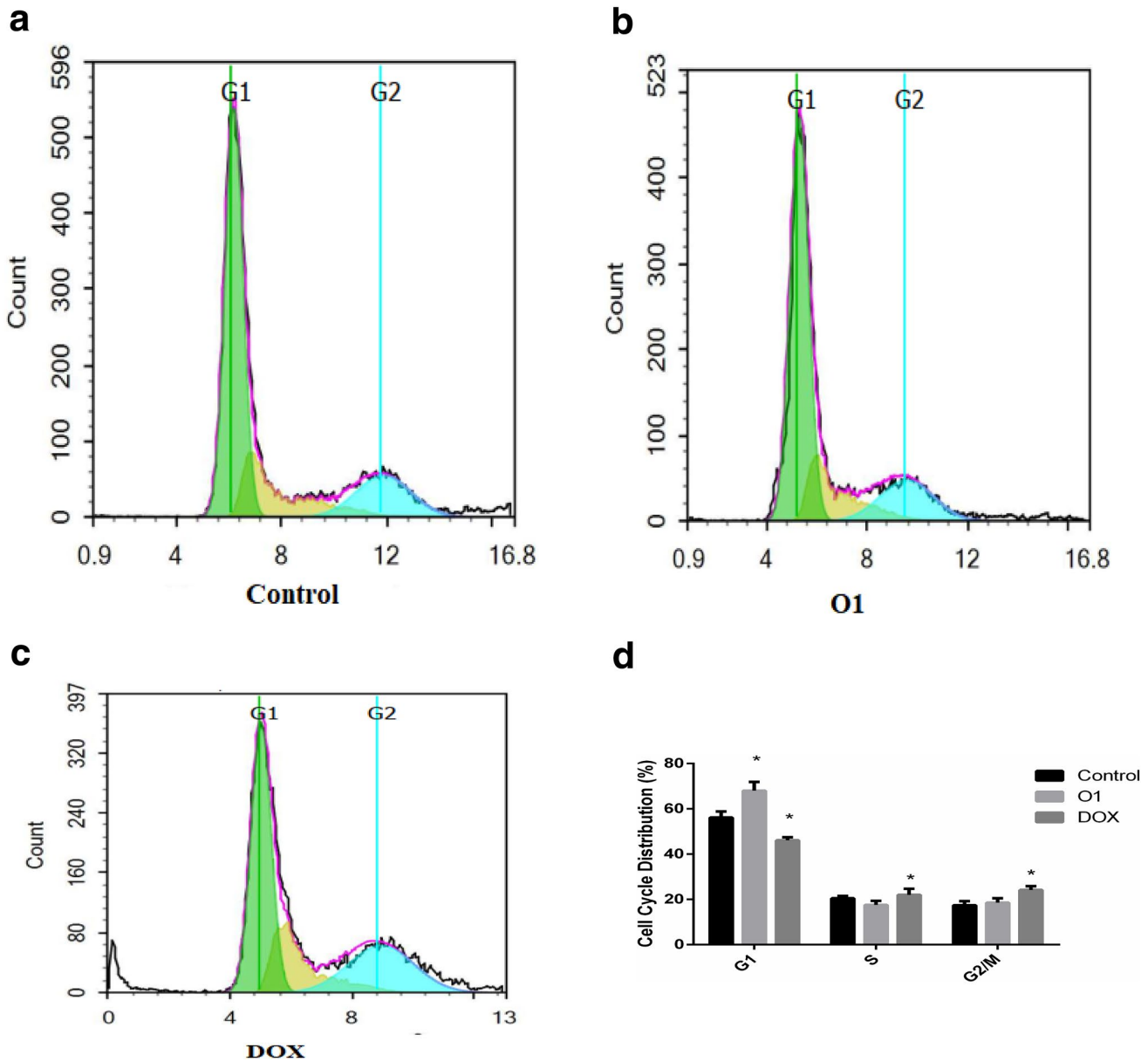

Fig. 5 Cell cycle analysis in HepG2 cells using flow cytometry. Representative histogram of the gated cells in the G0/G1, S, and G2/M phases for **a** control (untreated cells); **b** O_1 (optimized formula); **c** DOX. **d** Quantitative analysis of distribution or proportion of the cells in each phase was performed from at least 10,000 cells per sample. Data are expressed as mean ± standard deviation for triplicates within an individual experiment (*$p < 0.05$)

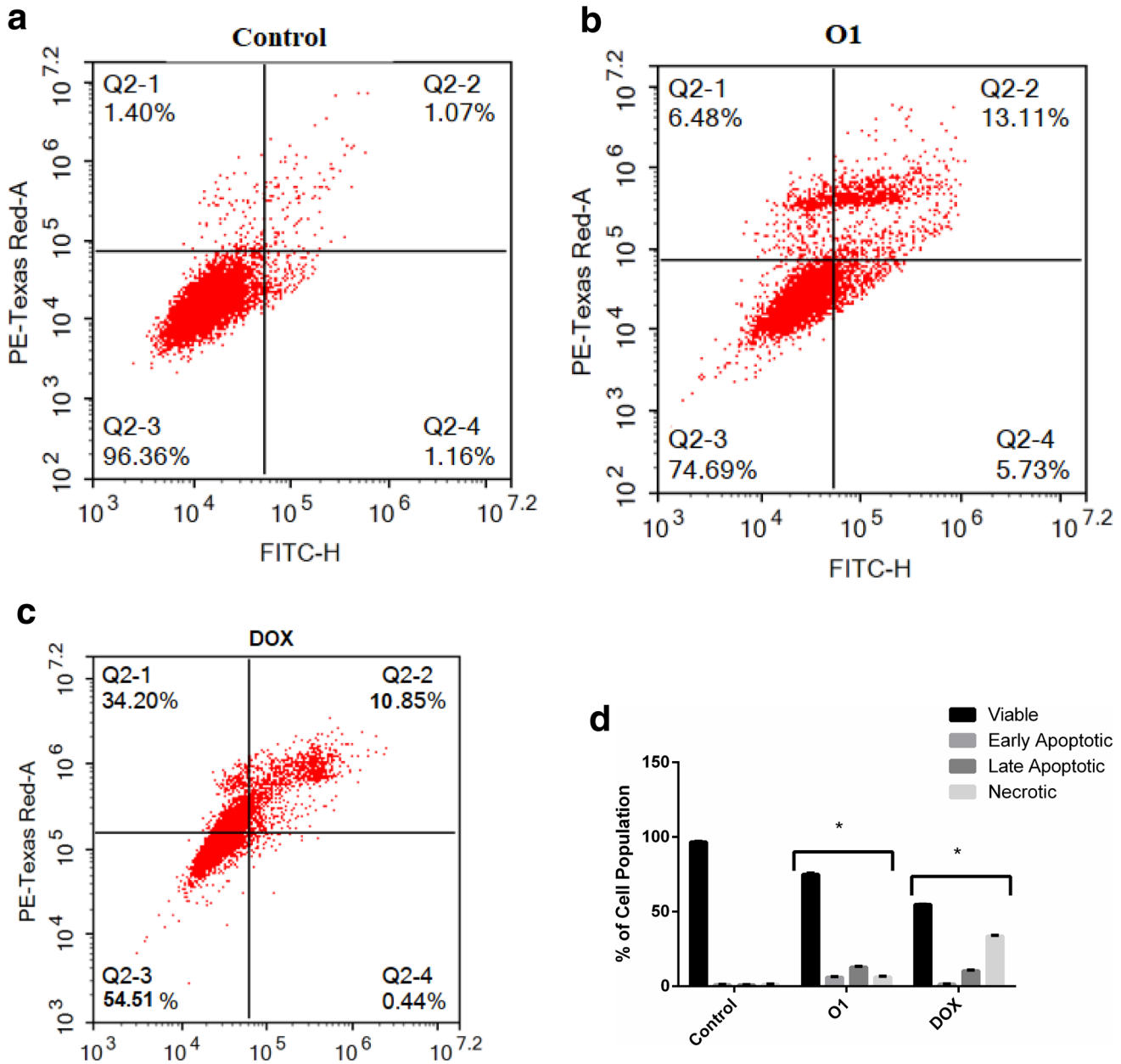

Fig. 6 Apoptosis analysis by Annexin-V/PI. Representative histogram of different cell population Viable, early apoptotic, late apoptotic and necrotic cells for **a** control (untreated cells; **b** O_1 (optimized formula); **c** DOX. **d** The percentage of cell population for evaluating the mode of cell death was estimated by using at least 10,000 cells per sample. Data are expressed as mean ± standard deviation for triplicates within an individual experiment (*$p < 0.05$)

to that of control untreated cells ($p < 0.05$). Using RSC in a nano-formulation enhances its anticancer activity as supported by Aldalaen et al. (2019) by triggering apoptosis, in addition to cell cycle arrest.

Apoptosis assay by flow cytometry

Carcinogenesis is usually mediated due to defect in apoptosis, which is programed cell death maintaining the healthy survival/death balance. Therefore, apoptosis is considered a molecular target in cancer therapy (Hassan et al. 2014). The apoptotic effect of O_1 formula was determined via an Annexin-V/PI based staining protocol. O_1 formula induced apoptotic cell death as indicated by the percentage of the early and late apoptotic cell population. Both apoptotic cell populations were significantly elevated as compared to control. In addition to apoptosis, O_1 formula enhanced necrotic cell death. On comparing O_1 formula with DOX, the

positive standard, cytotoxic effect of O_1 is mainly dependent on apoptotic mode of cell death, rather than necrosis (Fig. 6). Although, statins protect against inflammation and apoptosis in non-cancerous cells, as documented by several studies (Deng et al. 2015; Zhang et al. 2019), statins can induce cancer-specific apoptosis via mitochondrial apoptotic signaling pathways, triggered by the inhibition of biosynthesis of mevalonate or geranylgeranyl pyrophosphate (GGPP) (Hassanabad 2019).

Conclusion

Statins were found to have a potential anticancer activity, in addition to their well-known anti-hypercholesteremic effects. RSC is one of the potent statins that has been proved to have an anticancer activity, but it suffers poor bioavailability due to its poor solubility. Thus, the aim of the present study was to develop SNEDDS loaded with RSC, to overcome its delivery challenges and augment its anticancer activity.

In the present study, RSC-loaded SNEDDS were prepared and in vitro evaluated for the selection of the optimized formula. The optimized formula which was composed of 10% Peceol®, 45% Tween 80®, and 45% Trancutol ®P, showed a % transmittance of $99.05 \pm 0.09\%$, and a saturated solubility of 80.53 ± 2.57 mg/ml. The optimized SNEDDS formula showed a particle size of 17.53 ± 0.89 nm, with a zeta potential of − 10.2 mV. Transmission electron microscopy showed spherical shaped globules. In vitro drug release studies showed remarkable increase in the release of the optimized formula, as compared to the corresponding standard RSC, irrespective of the pH of the medium. It also suggested that the incorporation of RSC in SNEDDS could diminish the food effect. The optimized formula showed a significant enhancement in the cytotoxicity with IC_{50} value of 16.2 µg/ml, when compared to that of RSC (166.8 ± 5.33 µg/ml), indicating an enhanced cytotoxicity against HepG2 cells proliferation. The optimized formula affected cell cycle distribution, resulting in an arrest in G1 phase, as determined by cell cycle analysis. It also increased cell death by both apoptosis and necrosis, as evaluated by the flow cytometric analysis. Hence, SNEDDS composed of Peceol® as an oil, Tween 80® as a surfactant, and Transcutol® P as a cosurfactant, may provide a safe, potential, and effective drug delivery system for poorly soluble drugs, in order to enhance their solubility and anticancer activity.

Compliance with ethical standards

Conflict of interest The authors declare no conflict of interest.

Statement of human and animal rights This article does not contain any studies with human or animal subjects performed by any of the authors.

References

Abo Enin HA (2015) Self-nanoemulsifying drug-delivery system for improved oral bioavailability of rosuvastatin using natural oil antihyperlipidemic. Drug Dev Ind Pharm 41:1047–1056

AboulFotouh K, Allam AA, El-Badry M, El-Sayed AM (2017) Development and in vitro/in vivo performance of self-nanoemulsifying drug delivery systems loaded with candesartan cilexetil. Eur J Pharm Sci 109:503–513

Aldalaen S, El-Gogary RI, Nasr M (2019) Fabrication of rosuvastatin-loaded polymeric nanocapsules: a promising modality for treating hepatic cancer delineated by apoptotic and cell cycle arrest assessment. Drug Dev Ind Pharm 45:55–62

Avachat AM, Patel VG (2015) Self nanoemulsifying drug delivery system of stabilized ellagic acid-phospholipid complex with improved dissolution and permeability. Saudi Pharm J 23:276–289

Badran MM, Taha EI, Tayel MM, Al-Suwayeh SA (2014) Ultra-fine self nanoemulsifying drug delivery system for transdermal delivery of meloxicam: dependency on the type of surfactants. J Mol Liq 190:16–22

Baek IH, Kwon KI, Kim MS (2013) Effect of food on the pharmacokinetics of rosuvastatin after administration of a single oral dose in dogs. Drug Res (Stuttg) 63:145–149

Balakumar K, Raghavan CV, Selvan NT, Prasad RH, Abdu S (2013) Self nanoemulsifying drug delivery system (SNEDDS) of Rosuvastatin calcium: design, formulation, bioavailability and pharmacokinetic evaluation. Colloids Surf B 112:337–343

Basalious EB, Abdallah Ahmed M (2017) Phospholipid based self-nanoemulsifying self-nanosuspension (p-SNESNS) as a dual solubilization approach for development of formulation with diminished food effect: fast/fed in vivo pharmacokinetics study in human. Eur J Pharm Sci 109:244–252

Basalious EB, Shawky N, Badr-Eldin SM (2010) SNEDDS containing bioenhancers for improvement of dissolution and oral absorption of lacidipine. I: Development and optimization. Int J Pharm 391:203–211

Buggins TR, Dickinson PA, Taylor G (2007) The effects of pharmaceutical excipients on drug disposition. Adv Drug Deliv Rev 59:1482–1503

Chen M-L (2008) Lipid excipients and delivery systems for pharmaceutical development: a regulatory perspective. Adv Drug Deliv Rev 60:768–777

Ciofu C (2012) The statins as anticancer agents. Maedica 7(4):377

Craig DQM, Barker SA, Banning D, Booth SW (1995) An investigation into the mechanisms of self-emulsification using particle size analysis and low frequency dielectric spectroscopy. Int J Pharm 114:103–110

Cui J et al (2009) Enhancement of oral absorption of curcumin by self-microemulsifying drug delivery systems. Int J Pharm 371:148–155

Dash RN, Mohammed H, Humaira T, Ramesh D (2015) Design, optimization and evaluation of glipizide solid self-nanoemulsifying drug delivery for enhanced solubility and dissolution. Saudi Pharm J 23:528–540

Date AA, Desai N, Dixit R, Nagarsenker M (2010) Self-nanoemulsifying drug delivery systems: Formulation insights, applications and advances. Nanomed J 5:1595–1616

Deng J et al (2015) Rosuvastatin attenuates contrast-induced nephropathy through modulation of nitric oxide, inflammatory responses, oxidative stress and apoptosis in diabetic male rats. J Transl Med 13:53

El-Laithy HM, Basalious EB, El-Hoseiny BM, Adel MM (2015) Novel self-nanoemulsifying self-nanosuspension (SNESNS) for enhancing oral bioavailability of diacerein: simultaneous portal blood absorption and lymphatic delivery. Int J Pharm 490:146–154

Elnaggar YSR, El-massik MA, Abdallah OY (2009) Self-nanoemulsifying drug delivery systems of tamoxifen citrate: design and optimization. Int J Pharm 380:133–141

Fahmy UA, Ahmed OAA, Hosny KM (2014) Development and evaluation of avanafil self-nanoemulsifying drug delivery system with rapid onset of action and enhanced bioavailability. AAPS PharmSciTech 16:53–58

Garg B, Katare OP, Beg S, Lohan S, Singh B (2016) Systematic development of solid self-nanoemulsifying oily formulations (S-SNEOFs) for enhancing the oral bioavailability and intestinal lymphatic uptake of lopinavir. Colloids Surf B 141:611–622

Hassan M, Watari H, Abualmaaty A, Ohba Y, Sakuragi N (2014) Apoptosis and molecular targeting therapy in cancer. Biomed Res Int 2014:1–23

Hassanabad AF (2019) Current perspectives on statins as potential anticancer therapeutics: clinical outcomes and underlying molecular mechanisms. Transl Lung Cancer Res 8:692–699

Hong JY, Kim JK, Song YK, Park JS, Kim CK (2006) A new self-emulsifying formulation of itraconazole with improved dissolution and oral absorption. J Control Release 110:332–338

Hoshtari SZA, En JW, Ghassan R, Lany A (2010) Formulation and physicochemical characterization of Imwitor 308 based self microemulsifying drug delivery systems. Chem Pharm Bull 58:1332–1338

Isailović T et al (2016) Biocompatible nanoemulsions for improved aceclofenac skin delivery: formulation approach using combined mixture-process experimental design. J Pharm Sci 105:308–323

Jantratid E, Janssen N, Reppas C, Dressman JB (2008) Dissolution media simulating conditions in the proximal human gastrointestinal tract: an update. Pharm Res 25:1663–1676

Kassem AA, Mohsen AM, Ahmed RS, Essam TM (2016) Self-nanoemulsifying drug delivery system (SNEDDS) with enhanced solubilization of nystatin for treatment of oral candidiasis: design, optimization, in vitro and in vivo evaluation. J Mol Liq 218:219–232

Kommuru TR, Gurley B, Khan MA, Reddy IK (2001) Self-emulsifying drug delivery systems (SEDDS) of coenzyme Q10: formulation development and bioavailability assessment. Int J Pharm 212:233–246

Krstić M, Medarević Đ, Đuriš J, Ibrić S (2018) Self-nanoemulsifying drug delivery systems (SNEDDS) and self-microemulsifying drug delivery systems (SMEDDS) as lipid nanocarriers for improving dissolution rate and bioavailability of poorly soluble drugs. In: Lipid nanocarriers for drug targeting. William Andrew Publishing, pp 473–508.

Lawrence MJ, Rees GD (2012) Microemulsion-based media as novel drug delivery systems. Adv Drug Deliv Rev 64:175–193

Li Y et al (2007) Pharmacokinetic properties of rosuvastatin after single-dose, oral administration in chinese volunteers: a randomized, open-label, three-way crossover study. Clin Ther 29:2194–2203

Lind ML, Jacobsen J, Holm R, Müllertz A (2008) Intestinal lymphatic transport of halofantrine in rats assessed using a chylomicron flow blocking approach: the influence of polysorbate 60 and 80. Eur J Pharm Sci 35:211–218

Lu J, Wang J, Zhao S, Liu X, Zhao H (2008) Self-microemulsifying drug delivery system (SMEDDS) improves anticancer effect of oral 9-nitrocamptothecin on human cancer xenografts in nude mice. Eur J Pharm Biopharm 69:899–907

Mekhail GM, Kamel AO, Awad GAS, Mortada ND (2012) Anticancer effect of atorvastatin nanostructured polymeric micelles based on stearyl-grafted chitosan. Int J Biol Macromol 51:351–363

Mosmann T (1983) Rapid colorimetric assay for cellular growth and survival: application to proliferation and cytotoxicity assays. J Immunol Methods 65:55–63

Nankervis R, Davis SS, Day NH, Shaw PN (1996) Intestinal lymphatic transport of three retinoids in the rat after oral administration: effect of lipophilicity and lipid vehicle. Int J Pharm 130:57–64

Nepal PR, Han HK, Choi HK (2010) Preparation and in vitro-in vivo evaluation of Witepsol® H35 based self-nanoemulsifying drug delivery systems (SNEDDS) of coenzyme Q10. Eur J Pharm Sci 39:224–232

Parmar N, Singla N, Amin S, Kohli K (2011) Study of cosurfactant effect on nanoemulsifying area and development of lercanidipine loaded (SNEDDS) self nanoemulsifying drug delivery system. Colloids Surfaces B 86:327–338

Pouton CW, Porter CJH (2008) Formulation of lipid-based delivery systems for oral administration: materials, methods and strategies. Adv Drug Deliv Rev 60:625–637

Prajapat MD, Patel NJ, Bariya A, Patel SS, Butani SB (2017) Formulation and evaluation of self-emulsifying drug delivery system for nimodipine, a BCS class II drug. J Drug Deliv Sci Technol 39:59–68

Rahman MA, Mujahid M (2018) Development of self-nanoemulsifying tablet (SNET) for bioavailability enhancement of sertraline. Brazilian J Pharm Sci 54:1–14

Risovic V, Sachs-Barrable K, Boyd M, Wasan KM (2004) Potential mechanisms by which Peceol® increases the gastrointestinal absorption of Amphotericin B. Drug Dev Ind Pharm 30:767–774. https://doi.org/10.1081/DDC-120039793

Safwat S, Ishak RA, Hathout RM, Mortada ND (2017) Statins anticancer targeted delivery systems: re-purposing an old molecule. J Pharm Pharmacol 69:613–624

Salih OS, Samein LH, Ali WK (2013) Formulation and in vitro evaluation of rosuvastatin calcium niosomes. Int J Pharm Pharm Sci 5:525–535

Sandhu PS, Beg S, Mehta F, Singh B, Trivedi P (2015) Novel dietary lipid-based self-nanoemulsifying drug delivery systems of paclitaxel with p-gp inhibitor: Implications on cytotoxicity and biopharmaceutical performance. Expert Opin Drug Deliv 12:1809–1822

Savjani KT, Gajjar AK, Savjani JK (2012) Drug solubility: importance and enhancement techniques. Int Sch Res Not 2012:1–12

Senapati PC, Sahoo SK, Sahu AN (2016) Mixed surfactant based (SNEDDS) self-nanoemulsifying drug delivery system presenting efavirenz for enhancement of oral bioavailability. Biomed Pharmacother 80:42–51

Seo YG et al (2013) Development of docetaxel-loaded solid self-nanoemulsifying drug delivery system (SNEDDS) for enhanced chemotherapeutic effect. Int J Pharm 452:412–420

Shafiq S et al (2007) Development and bioavailability assessment of ramipril nanoemulsion formulation. Eur J Pharm Biopharm 66:227–243

Shahba AAW, Mohsin K, Alanazi FK (2012) Novel self-nanoemulsifying drug delivery systems (SNEDDS) for oral delivery of cinnarizine: design, optimization, and in-vitro assessment. AAPS PharmSciTech 13:967–977

Shakeel F, Haq N, Alanazi FK, Alsarra IA (2014) Polymeric solid self-nanoemulsifying drug delivery system of glibenclamide using coffee husk as a low cost biosorbent. Powder Technol 256:352–360

Shen H, Zhong M (2006) Preparation and evaluation of self-microemulsifying drug delivery systems (SMEDDS) containing atorvastatin. Acta Pharm Sin 58:1183–1191

Shukla M et al (2017) A combination of complexation and self-nanoemulsifying drug delivery system for enhancing oral bioavailability and anticancer efficacy of curcumin. Drug Dev Ind Pharm 43:847–861

Singh SK, Prasad Verma PR, Razdan B (2010) Glibenclamide-loaded self-nanoemulsifying drug delivery system: development and characterization. Drug Dev Ind Pharm 36:933–945

Soltani Y, Goodarzi N, Mahjub R (2017) Preparation and characterization of self nano-emulsifying drug delivery system (SNEDDS) for oral delivery of heparin using hydrophobic complexation by cationic polymer of β-cyclodextrin. Drug Dev Ind Pharm 43:1899–1907

Tripathi CB et al (2018) ω-3 fatty acid synergized novel nanoemulsifying system for rosuvastatin delivery. In vitro and in vivo evaluation. AAPS PharmSciTech 19:1205–1218

Ujilestari T, Martien R, Ariyadi B, Dono ND, Zuprizal (2018) Self-nanoemulsifying drug delivery system (SNEDDS) of Amomum compactum essential oil: design, formulation, and characterization. J Appl Pharm Sci 8:14–21

Umeyor C et al (2016) Formulation design and in vitro physicochemical characterization of surface modified self-nanoemulsifying formulations (SNEFs) of gentamicin. Int J Pharm 497:161–198

U.S. Food and Drug Administration (2019) Drugs@FDA: FDA-Approved Drugs. In: U.S. Food Drug Adm.

Wang Z et al (2010) Solid self-emulsifying nitrendipine pellets: preparation and in vitro/in vivo evaluation. Int J Pharm 383:1–6

Zhang P-X, Zhang H-X, Hou D-L, Xiao Z-C, Zhou C-Y (2019) Cardioprotection of rosuvastatin pre-conditioning on myocardial ischemia / reperfusion injury in a rat model. Braz Arch Biol Technol 62:1–12

Zhao Y et al (2010) Self-nanoemulsifying drug delivery system (SNEDDS) for oral delivery of Zedoary essential oil: formulation and bioavailability studies. Int J Pharm 383:170–177